24th INTERNATIONAL CONGRESS ON SOUND AND VIBRATION
23–27 July 2017, London

PREDICTION AND ANALYSIS OF FRICTION-INDUCED NOISE IN ELASTOMERIC BEARINGS

Neng Zhang, Lin He and Xue Yang

National Key Laboratory on Ship Vibration and Noise, Institute of Noise and Vibration, Naval University of Engineering, Wuhan 430033, China

email:zn710119@163.com

Friction-induced noise in elastomeric bearings originates from unstable contact force between shaft and rubber bearing facing. A finite element model of elastomeric bearing system is established and complex eigenvalue analysis is applied with ABAQUS. A qualitative evaluation indicator is introduced to represent friction-induced noise in a certain frequency range. Effects of rotational speed of shaft, specific pressure and elasticity of rubber on friction-induced noise are analyzed and predicted.

Keywords: elastomeric bearing, friction-induced noise, complex eigenvalue analysis, qualitative evaluation indicator, distribution of eigenvalues

1. Introduction

Elastomeric bearings are extensively used in marine propulsion system. The structure of elastomeric bearings is shown in Fig. 1. Lubricated by seawater, elastomeric bearings are pollution-free, self-sufficient and high-performance [1]. However, friction-induced noise in elastomeric bearings is one of the most troublesome concerns in acoustic stealth of underwater vehicles [2-4].

Friction between contacting interfaces leads to irregular motion, thus resulting unwanted sound, which has been widely studied these years. Although frictional mechanical behaviour and contact characteristics have been elaborated through numerous experiments and various friction models are summarized [5-7], friction-induced noise, so-called squeal or squeak, is still obscure and difficult to analyze and predict quantitatively.

Acoustics of friction and friction-induced vibrations and waves in solids have been systematically and extensively expounded by Adnan Akay [8]. At the microcosmic scale, friction develops a mechanism that converts the kinetic energy between contact interfaces and leads to atomic random motion. Three different friction-induced noise categories—squeal, squeak and creak noises are characterized and explained with a phenomenological model [9]. And three main physical mechanisms related to each kind of noise are found: the slick-slip, the sprag-slip and the mode-coupling instabilities. However, their researches lay particular emphasis on microcosmic phenomena and the mechanism of friction-induced noise.

Heated investigation subjects related to friction-induced noise mainly comprise rail-wheel noise, automotive brake squeal and journal bearing noise. Effects of lateral creepage and stick coefficient on rail-wheel noise are studied [10] and rail-wheel noise characteristics are summarized [11, 12]. Brake squeal is predicted via complex eigenvalue method to facilitate mechanical design of brake disc and pad [13-16]. As to journal bearing, self-excited vibration mechanism is investigated to account for friction-induced noise in water-lubricated bearing with a two DOF system [2, 3]. In [17, 18], effects of structure parameters and friction coefficient on friction-induced noise in water-lubricated bearing are illustrated. However, the tendency and intensity of friction-induced noise

under different working conditions in elastomeric bearing are not investigated theoretically yet. Besides, characteristics of friction-induced noise in different frequency range are not clear and no qualitative indicator is introduced to evaluate it.

In this paper, friction-induced noise of elastomeric bearing is analyzed and predicted. Firstly, complex eigenvalue extraction theory is introduced. Then, an elastomeric bearing system including shaft, rubber bearing facing and copper bushing is established via FEM. Procedures to analyze and predict friction-induced noise are detailed. Finally, through illustrations of distribution of complex eigenvalue in frequency domain and qualitative indicator to represent friction-induced noise, effects of rotational speed of shaft, specific pressure and elasticity of rubber on friction-induced noise are analyzed and predicted.

2. General style parameters

2.1 Complex eigenvalue extraction

According to [18], the motion equation of elastomeric bearing system model can be written as

$$\mathbf{M}\{\ddot{\mathbf{x}}\} + \mathbf{C}\{\dot{\mathbf{x}}\} + (\mathbf{K} - \mathbf{K_f})\{\mathbf{x}\} = \{\mathbf{0}\} \quad (1)$$

where M、C、K are system mass matrix, damping matrix and initial stiffness matrix, respectively. $\mathbf{K_f}$ is coupling stiffness matrix induced by tangential friction and normal displacement between elastomeric bearing and shaft.

$\mathbf{K_f}$ is unsymmetrical, which is prone to external energy feed into the system to a certain extent, leading to system unstability. In order to analyze instability of the system and thus predict friction-induced noise, complex eigenvalue extraction method is introduced. The basic procedure of the method is as follows.

$$\left(\boldsymbol{\lambda}^2\mathbf{M} + \boldsymbol{\lambda}\mathbf{C} + \mathbf{K} - \mathbf{K_f}\right)\boldsymbol{\Phi} = \{0\} \quad (2)$$

where λ is the eigenvalue and Φ is the corresponding eigenvector.

As eigenvalues and eigenvectors may be complex, it is difficult to solve Eq. (2) directly. Here projection subspace method is adopted. Real eigenvalues and eigenvectors are solved first by ignoring damping matrix as well as unsymmetrical stiffness matrix. Thus projection subspace is acquired and composed of real eigenvectors denoted in a matrix as $[\psi_1,\ \psi_2,\ \cdots\psi_N]$. The matrices in Eq. (2) are projected onto the subspace

$$\mathbf{C}^* = [\psi_1,\ \psi_2,\ \cdots\psi_N]^{\mathrm{T}}\mathbf{C}[\psi_1,\ \psi_2,\ \cdots\psi_N] \quad (3)$$

$$\mathbf{K}^* = [\psi_1,\ \psi_2,\ \cdots\psi_N]^{\mathrm{T}}\mathbf{K}[\psi_1,\ \psi_2,\ \cdots\psi_N] \quad (4)$$

$$\mathbf{K_f}^* = [\psi_1,\ \psi_2,\ \cdots\psi_N]^{\mathrm{T}}\mathbf{K_f}[\psi_1,\ \psi_2,\ \cdots\psi_N] \quad (5)$$

After projection, the characteristic equation can be rewritten as

$$(\lambda^2\mathbf{M}^* + \lambda\mathbf{C}^* + \mathbf{K}^* - \mathbf{K_f}^*)\boldsymbol{\Phi}^* = \{0\} \quad (6)$$

Finally, complex eigenvalues and eigenvectors can be obtained by projecting to the subspace

$$\boldsymbol{\Phi} = [\psi_1,\ \psi_2,\ \cdots\psi_N]^{\mathrm{T}}\boldsymbol{\Phi}^* \quad (7)$$

A certain complex eigenvalue can be expressed as

$$\lambda = \alpha + j\omega \quad (8)$$

The solution corresponding to this eigenvalue is

$$x = e^{\alpha t}(A_1 cos\omega t + A_2 sin\omega t) \quad (9)$$

Thus general solution of Eq. (1) is

$$x = \sum_{i=1}^{N} e^{\alpha_i t}[A_1(i)cos\omega_i t + A_2(i)sin\omega_i t] \quad (10)$$

where α and ω are the real part and imaginary part of λ. ω denotes the mode frequency and α is relevant to instability of the system. The system becomes unstable when α is positive, thus leading to friction-induced noise.

Therefore, characteristics of friction-induced noise can be represented by eigenvalues [19].

2.2 Finite element model

2.2.1 Model description

FE model of the elastomeric bearing system is shown in Fig. 2, which is made up of shaft, rubber bearing facing and copper bushing. Rubber bearing facing is completely constrained at its outer cylinder surface and copper bushing is tied to rubber bearing facing. The shaft can only rotate and other DOFs are constraint. There are 8 grooves in axial direction inside the rubber bearing facing to let lubrication water in and out. Geometrical parameters of the elastomeric bearing system are shown in Table 1.

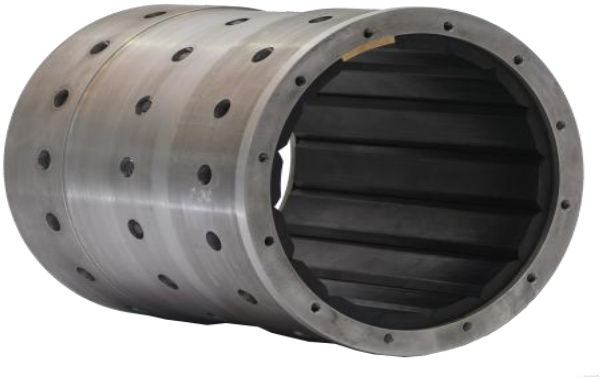

Figure 1: Structure of the elastomeric bearings

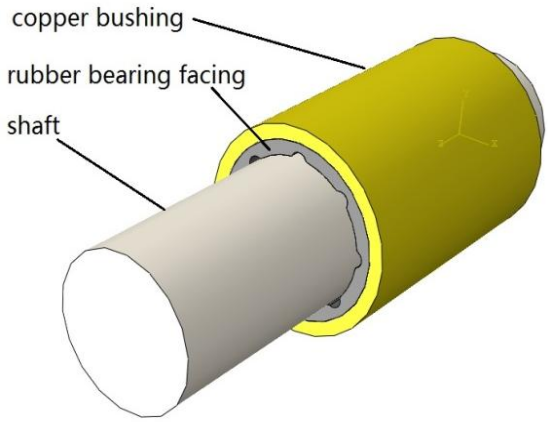

Figure 2: FE model of elastomeric bearing system

Table 1: The geometry parameters of the elastomeric bearing system

Geometry parameters (mm)	Value
Length of rubber bearing facing	100
Thickness of copper bushing	5
External diameter of rubber bearing facing	70
Internal diameter of rubber bearing facing	50
Radius of the grooves	3
Radius of transition arc	1

2.2.2 Analysis procedures

With FE model of the elastomeric bearing system developed, the procedures to apply ABAQUS to perform complex eigenvalue extraction are as follows:

(1) Nonlinear static analysis to define and specific pressure.
(2) Another nonlinear static analysis to apply rotational speed of shaft.
(3) Normal modal analysis to extract real eigenvalue and natural mode in order to find the projection subspace.
(4) Complex eigenvalue analysis with the effect of friction coupling considered to obtain complex eigenvalue.

3. Results and discussion

3.1 Friction model and introduction of impact factor of friction-induced noise

According to [20], relative velocity-dependent friction model described as exponential formulation is adopted to represent sliding contact between rubber bearing facing and shaft. As is shown in Fig. 3, the friction coefficient is denoted as

$$\mu = \mu_d + (\mu_s - \mu_d)e^{-\zeta v_r} \tag{11}$$

In Eq. (11), μ_d and μ_s are dynamic friction coefficient and static friction coefficient respectively and ζ is decaying factor. They are assumed to be: μ_d=0.2, μ_s=0.3 and ζ=1. v_r denotes the relative velocity of contact interfaces of shaft and the elastomeric bearing facing.

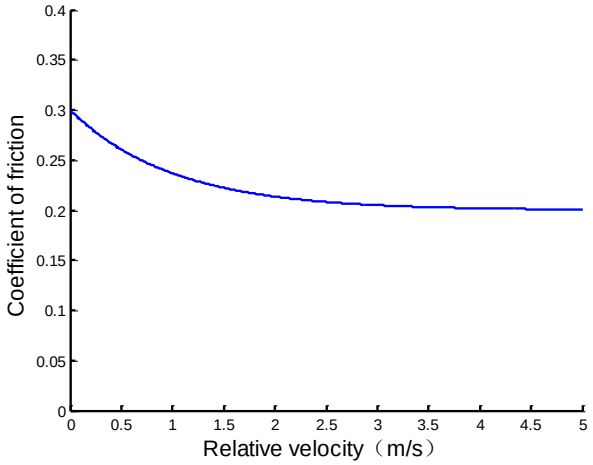

Figure 3: Friction coefficient-relative velocity curve

Here, rubber is assumed to be linear elastic because nonlinearity is ignored in complex eigenvalue analysis [19]. Material parameters of shaft, rubber bearing facing and copper bushing shown in Table 2 are available for the following analysis 3.2 and 3.3. Effect of elastic modulus of rubber on friction-induced noise will be investigated in 3.4 so the value of elastic modulus of rubber bearing facing will be altered there.

Table 2: The parameters of materials of bearing system

Components	Elastic Modulus (Pa)	Poisson Ratio	Density (kg/m^3)
Shaft	2.1×10^{11}	0.3	7800
Rubber bearing facing	7.8×10^{6}	0.47	1500

Negative eigenvalues imply system stability, while positive eigenvalues imply system instability and lead to friction-induced noise in elastomeric bearing system. In order to predict and analyze friction-induced noise quantitatively, contributions of all positive eigenvalues on friction-induced noise need to be considered. Here exponential summation of all positive eigenvalues is calculated and a specific index termed impact factor of friction-induced noise is introduced

$$\Psi = \sum_{i=1}^{n} e^{\xi \alpha_i} \tag{12}$$

In Eq. (12), Ψ denotes impact factor of friction-induced noise. ξ is a constant coefficient, and equals 1×10^{12} here for the sake of data processing and calculation convenience. α_i is real part of the ith positive eigenvalue and n is total number of positive eigenvalues. According to [8], the frequency range of friction-induced noise between rubber and metal is 1.5kHz-3.0kHz. Here, this frequency range is adopted and is divided equally into three regions 1.5kHz-2.0kHz, 2.0kHz-2.5kHz and 2.5kHz-3.0kHz. Ψ_1, Ψ_2 and Ψ_3 represent impact factor of friction-induced noise in each region, respectively. From the formula, it is easily concluded that contributions of all positive eigenvalues to friction-induced noise are weighed.

Rotational speed of shaft and specific pressure in elastomeric bearings are key working condition parameters and elastic modulus of rubber is one of the most important material parameters. Effects of these three parameters are investigated via FEM and complex eigenvalue data analysis below.

3.2 Effect of rotational speed of shaft

This part deals with the effect of rotation speed of shaft on friction-induced noise in the elastomeric bearing system. In the simulation, the specific pressure is set to 0.3MPa and three

different rotational speed values of shaft applied are 20r/min, 60r/min and 100r/min. Distribution of unstable complex eigenvalues in the frequency domain impact factors of friction-induced noise in different frequency range are illustrated in Fig. 4 and Tab 3, respectively.

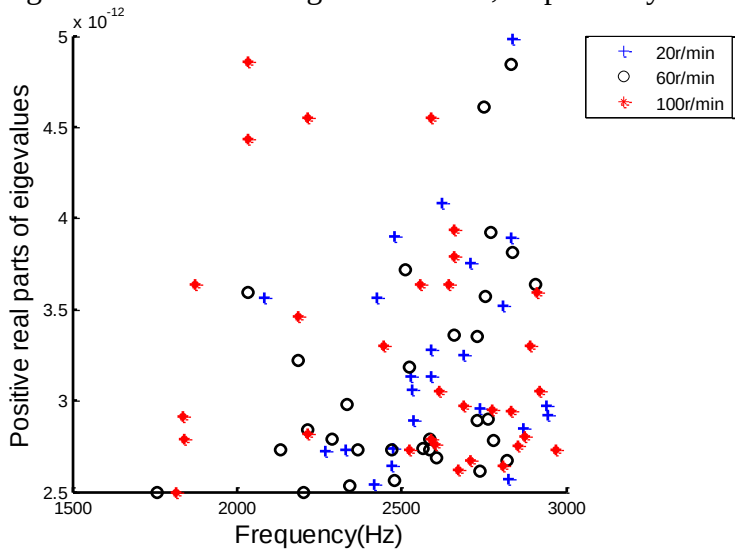

Figure 4: Distribution of unstable complex eigenvalue under different rotational speeds

Fig. 4 shows that almost all unstable eigenvalues spread in 2.0kHz-2.5kHz and 2.5kHz-3.0kHz when rotational speed is 20r/min. When rotational speed rises up to 60r/min, most of unstable eigenvalues spread in 2.5 kHz-3.0 kHz. And unstable eigenvalues scatter in 1.5kHz-2.0kHz, 2.0kHz-2.5kHz and 2.5kHz-3.0kHz three regions when rotational speed is up to 100r/min. The majority of unstable eigenvalues appear in 2.5kHz-3.0kHz.

Table 3: Relationship between factor of friction-induced noise and rotational speed

Rotational Speed (r/min)	Ψ_1 (1.5-2.0kHz)	Ψ_2 (2.0-2.5kHz)	Ψ_3 (2.5-3.0kHz)
20.00	57.54	957.83	5921.82
60.00	72.89	455.89	5206.44
100.00	149.44	1217.45	2875.78

As is shown in Table 3, impact factor of friction-induced noise rises as rotational speed rises from 20r/min to 100r/min. What's more, the magnitude of this index reflects that friction-induced noise appears extensively in 2.5kHz-3.0kHz and the energy of friction-induced noise is shifting towards lower frequency when rotational speed rises from 20 r/min to 100 r/min. This trend accords with distribution characteristics of unstable eigenvalues under different rotational speeds.

3.3 Effect of specific pressure

In order to investigate the effect of specific pressure on friction-induced noise in the elastomeric bearing system, rotational speed is kept 20r/min all the time. Three different specific pressure values applied in the simulation are 0.3MPa, 0.6MPa and 0.9MPa. Distribution of unstable eigenvalues in frequency domain and impact factors of friction-induced noise are shown in Fig. 5 and Table 4, respectively.

It is concluded from Fig. 5 that most unstable eigenvalues spread in 2.0kHz-2.5kHz and 2.5kHz-3.0kHz for different specific pressure values and no unstable eigenvalue appears in 1.5kHz-2.0kHz until specific pressure rises to 0.9MPa.

Table 4 shows that impact factor of friction-induced noise in 1.5kHz-2.0kHz rises as the specific pressure rises from 0.3MPa to 0.9MPa. The magnitude implies that friction-induced noise occurs mostly in 2.5kHz-3.0kHz.

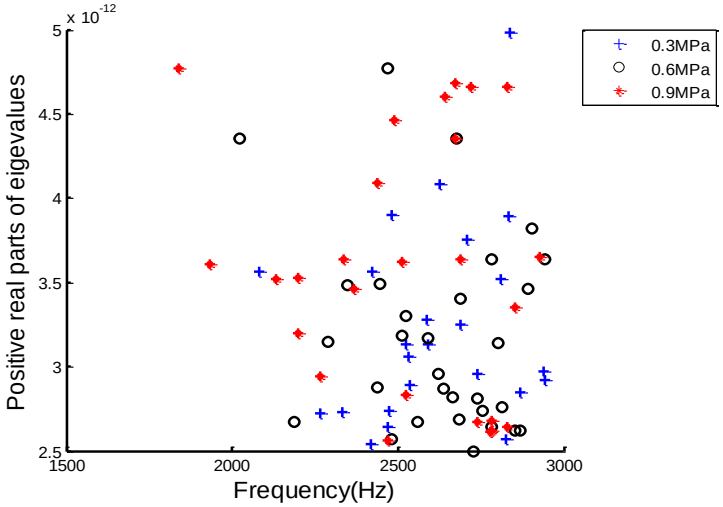

Figure 5: Distribution of unstable complex eigenvalue under different specific pressure values

Table 4: Relationship between factor of friction-induced noise and specific pressure

Specific Pressure (MPa)	Ψ_1 (1.5-2.0kHz)	Ψ_2 (2.0-2.5kHz)	Ψ_3 (2.5-3.0kHz)
0.30	57.54	957.83	5921.82
0.60	107.47	589.47	3601.06
0.90	796.37	650.74	6554.98

3.4 Effect of elastic modulus of rubber

In this part, rotational speed is kept 20r/min and the specific pressure is 0.3MPa. The parameter of elastic modulus of rubber in Table 2 is not available and simulations are conducted under three different values—4MPa, 6MPa and 8MPa. Other material parameters remain unchanged. Distribution of unstable eigenvalues in frequency domain and impact factors of friction-induced noise are shown in Fig. 6 and Table 5.

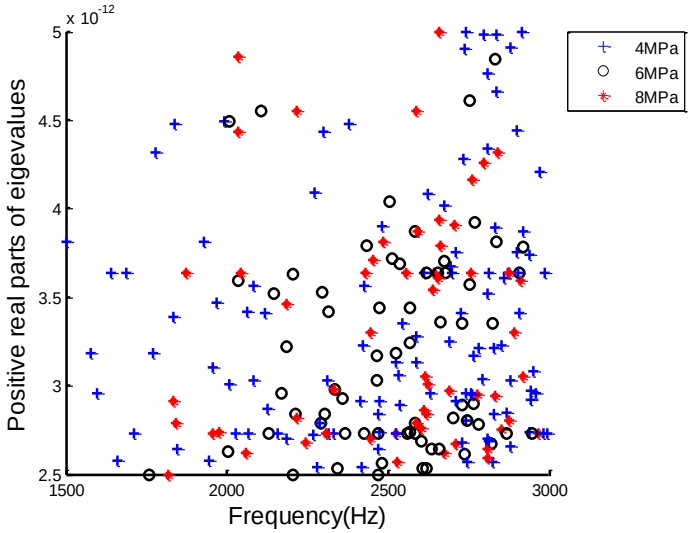

Figure 6: Distribution of unstable complex eigenvalue with different elasticity of rubber values

As is shown in Fig. 6, unstable eigenvalues scatter in 1.5kHz-2.0kHz, 2.0kHz-2.5kHz and 2.5kHz-3.0kHz when the value of elastic modulus of rubber is 4MPa. And overwhelming majority of unstable eigenvalues spread in 2.0kHz-2.5kHz and 2.5kHz-3.0kHz when it rises to 6MPa and 8MPa. In addition, number of unstable eigenvalue decreases as the value of elastic modulus of rubber rises from 4MPa to 8MPa.

Table 5: Relationship between factor of friction-induced noise and elasticity of rubber

Elasticity of Rubber (MPa)	Ψ_1 (1.5-2.0kHz)	Ψ_2 (2.0-2.5kHz)	Ψ_3 (2.5-3.0kHz)
4.00	2088.01	1912.22	238195.04
6.00	179.42	2582.54	6990.97
8.00	101.63	508.36	122181.96

Table 5 implies impact factor of friction-induced noise in 1.5kHz-2.0kHz decreases as the value of elastic modulus of rubber rises from 4MPa to 8MPa. Besides, judging from the magnitude of impact factor of friction-induced noise, friction-induced noise mostly occurs in 2.5kHz-3.0kHz. Impact factor of friction-induced noise is quite small when the value of elastic modulus of rubber is 6MPa. 6MPa is almost the optimal value of elastic modulus for rubber for the elastomeric bearing system in this paper. It is concluded that rubber with the optimal value of elastic modulus is beneficial to attenuation of friction-induced vibration and noise.

4. Conclusion

This paper deals with analyzing and predicting friction-induced noise in elastomeric bearing system with ABAQUS. Impact factor of friction-induced noise is introduced as a qualitative evaluating indicator to predict noise in a certain frequency range. Effects of rotational speed of shaft, specific pressure and elasticity of rubber on friction-induced noise are elaborated. The conclusions are as follows:

1. Impact factor of friction-induced noise increases as rotational speed rises.
2. The energy of friction-induced noise is shifting towards lower frequency when rotational speed rises.
3. Impact factor of friction-induced noise in 1.5kHz-2.0kHz rises as specific pressure rises. According to the magnitude of impact factor, friction-induced noise occurs mostly in 2.5kHz-3.0kHz for different specific pressure values.
4. 6MPa is almost the optimal value of elastic modulus of rubber for the elastomeric bearing system in this paper. For a specific elastomeric bearing, selecting rubber with optimal value of elastic modulus as bearing facing material is beneficial to attenuation of friction-induced vibration and noise.

REFERENCES

1 Wojciech Litwin. Water lubricated marine stern tube bearings-attempt at estimating hydrodynamic capacity. *Proceedings of ASME/STLE International Joint Tribology Conference*, America, (2009).

2 Simpson T A and Ibrahim R A. Nonlinear friction-induced vibration in water-lubricated bearings. *Journal of Vibration and Control*, **4**(1), 87- 113, (1996).

3 Ibrahim R A. Friction-induced vibration, chatter, squeal and chaos, Part I: mechanics of contact friction. *ASME Applied Mechanics Review*, **47**(7), 209-226, (1994).

4 A I Krauter. Generation of squeal/chatter in water-lubricated elastomeric bearing. *Journal of lubrication Technology*, **103**(3), 406-413, (1981).

5 Choong-Min Jung. *Friction-induced vibration in linear elastic media with distributed contact*, PhD Thesis, Michigan State University, (1999).

6 Jianxun Liang. *Contact dynamics with model order reduction and application*, PhD Thesis, New Mexico State University, (2012).

7 Jamil A. Abdo. *Contact characteristics and their contributions to dynamic instability of mechanical systems with friction*, PhD Thesis, Southern Illinois University, (2000).

8 Adnan Akay. Acoustics of friction. *Acoustical Society of America*, **111**(4), 1525-1548, (2002).

9 A Elmaian，F Gautier，C Pezerat, et al. How Can Automotive Friction-induced Noises Be Related to Physical Mechanisms. *Applied Acoustics*, **76**(1), 391-401, (2014).

10 A. D. Monk-Steel, D. J. Thompson and F. G. de Beer. An investigation into the influence of longitudinal creepage on railway squeal noise due to lateral creepage. *Journal of Sound and Vibration*, **293**(3), 766-776, (2006).
11 N. Vineent, J. R. Koch, H. Chollet, et al. Curve squeal of urban rolling stock-Part l: State of the art and field measurements. *Journal of Sound and Vibration*, **293**(3), 691-700, (2006).
12 Eadie D T and Santoro M. Top-of-rail friction control for curve noise mitigation and corrugation rate reduction. *Journal of Sound and Vibration*, **293**(3), 747-757, (2006).
13 Heewook Lee. *An optimal design method for brake squeal noise based on complex eigenvalue and sensitivity analyses and response surface methodology*, PhD Thesis, University of Michigan, (2000).
14 P. Liu, H. Zheng, C. Cai，et al. Analysis of disc brake squeal using the complex eigenvalue method. *Applied Acoustics*, **68**(6), 603–615, (2007).
15 Abd Rahim AbuBakar and Huajiang Ouyang. Complex eigenvalue analysis and dynamic transient analysis in predicting disc brake squeal. *International Journal of Vehicle Noise and Vibration*, **2**(2), 143-155, (2006).
16 M. Nouby, D. Mathivanan and K. Srinivasan. A combined approach of complex eigenvalue analysis and design of experiments (DOE) to study disc brake squeal. *International Journal of Engineering*, Science and Technology, **1**(1), 254-271, (2009).
17 Wang Jiaxu, Liu Jing, Xiao Ke, et al. Analysis of friction-induced noise in water-lubricated bearings with different structures. *Mechanical Transmission*, **35**(9), 12-14, (2011).
18 Liu Wenhong. *Analysis of vibration noise of water-lubricated rubber bearings and experiment research*, Master of Science Thesis, Chongqing University, (2012).
19 ABAQUS 6.10 Analysis User's Manual, **5**, (2010).
20 Timothy C. Ovaert, Herbert S. Cheng and Harold H. Kantner. Tribological characteristics of elastomeric and elastomeric/thermoplastic contacts under conformal sliding conditions. *Wear and friction of elastomers*, ASTM STP 1145, (1991).